Light Metals 2014
Edited by: John Grandfield
TMS (The Minerals, Metals & Materials Society), 2014

A CFD-PBM COUPLED MODEL PREDICTING ANODIC BUBBLE SIZE DISTRIBUTION IN ALUMINUM REDUCTION CELLS

Shuiqing Zhan[1], Mao Li[1,2], Jiemin Zhou[1], Jianhong Yang[3], Yiwen Zhou[3], Chenn Q Zhou[2],
[1]School of Energy Science and Engineering, Central South University, Changsha 410083, Hunan, China;
[2]Center for Innovation through Visualization and Simulation, Purdue University Calumet, Hammond, IN46323, USA;
[3]Zhengzhou Research Institute, CHALCO Ltd, Zhengzhou 450041, Henan, China

Keywords: aluminum reduction cells, multiphase flow, population balance model, bubble size distribution

Abstract

In order to understand more details of anodic bubble formation, coalescence and movement mechanism under the horizontal anode bottom, a population balance model (PBM) was used to calculate the anodic bubble size distribution (BSD) in aluminum reduction cells. The proposed PBM was numerically solved with a class method (CM) which has been provided in ANSYS FLUENT. A CFD-PBM coupled model that combines the PBM and CFD model was used to simulate more complex flow behavior with proper coalescence and breakage mechanism of anodic bubble. A modified k-ε turbulence model was used to describe liquid phase turbulence in the simulation. The effects of current density, anode width and the presence of slots on the BSD have been investigated. In addition, the relative influence of the bath flow induced by the cell magneto-hydrodynamic (MHD) on the BSD is also discussed. The predicted BSD is in accordance with a series of literature experimental results.

Introduction

During the operation of commercial aluminum reduction cells, anodic bubble (mainly carbon dioxide) is generated under the anode bottom, and move up through the bath under the influence of buoyancy, recirculation flows. The anodic bubble induces bath flow in the cell which plays an important positive role in homogenization of the alumina distribution and temperature field. Due to the large area of the anode, the anodic bubbles gradually gather under the anode bottom, therefore, the phenomenon of coalescence and breakage can often occur between bubbles, which can produce some bubble group with different sizes, forming a certain thickness of the bubble layer. Conversely, the bubbles increase voltage drop under the anode bottom which in turn results in high energy consumption during the electrolytic process.

The previous studies of anodic bubble distribution characteristics are mainly focused on three aspects: the physical modeling, electrolytic test and numerical simulation. Fortin et al. [1] was the first to use a full-scale water model to study the effects of some key operating parameters i.e., current density, anode-cathode distance and anode inclination angle on the bubble layer, anode bubble coverage and bubble release frequency. Solheim et al. [2] found that bubble size decreased with the addition of propanol which inhibits the coalescence. It was reported that the small bubble results in high accumulated gas volume as well as high resistivity in the bubble layer. Xiang-peng L et al. [3] reported that bubble size increased with an increase in liquid surface tension and decreased at high anode inclination angle. Qian and Chen [4-6] presented a comprehensive review of the phenomenon of bubble formation, coalescence, breakage and movement mechanism under the horizontal anode bottom and found that there was a strong relationship between the anodic bubble size distribution and anode material, spatial position(anode bottom or side channel) and the operation parameters.

In summary, it is clear that the initial bubbles generated under the anode bottom are very small and generally uniform in size. The existence of these small and uniform bubbles can form more and more large bubbles, which have an important influence on the electrolysis process. Physical modeling using the compressed air as the anode gas is not perfect due to restriction on experimental condition, where the mechanism of the generated gas is different from electrochemical reaction. On the other hand, the spatial bubble size distribution of electrolytic test system dose not apply to real industrial aluminum reduction cells because of small scale of the model (10-20mm) as compared with that of the real cells. Although there have already been more and more studies on the experiments, a lot of key problems are still remaining unsolved. Neither small scale electrolysis test nor real scale water-air model can reproduce correctly the morphology and the dynamics of the bubble size distribution in aluminum reduction cells.

Many numerical simulations based on the prediction of complex gas-liquid flows were also used to study aluminum reduction cells system with different focuses. There are several methods available for the mathematical modeling of two-or multiphase flow, i.e., the volume of fluid (VOF) method, the Euler-Euler method and Euler-Lagrange method [7-10]. To some extent, these methods could predict the multiphase flow field and the bubble volume fraction or size distribution based on constant bubble size modeling, but could not obtain real bubble size distribution. Owing to the fundamental importance of bubble size in anodic bubble-bath flows, the predictions of bubble size distribution become very important for the understanding of the hydrodynamics of aluminum reduction cells. Moreover, the bubble size under the anode bottom is dependent on local turbulence intensities as they directly affect the bubble coalescence and breakage phenomena.

In recent years, there have been a number of studies [11-14] using population balance model(PBM) to calculate the distribution of bubbles with gas-liquid two-phase Euler-Euler model by considering bubble coalescence and breakage phenomena. At present, the most widely used in industry is bubble columns, where many valuable conclusions have been provided. To date, however, we have yet to see any studies on taking into account the coalescence and breakage of anodic bubbles in aluminum reduction cells. We have used a two-fluid Euler-Euler model with constant bubble size for the calculation of interfacial forces in the governing equations of CFD previously [15]. In the present work, a CFD-PBM coupled model that combines the PBM and CFD model was used to simulate more complex anodic bubble/bath

two phase flow behavior with proper coalescence and breakage mechanism of anodic bubbles. And the effects of current density, anode width and the presence of slots on the bubble size distribution have been investigated. In addition, the relative influence of the bath flow induced by the cell magneto-hydrodynamic (MHD) on the BSD is also discussed.

Modeling approach

CFD modeling of two-phase flow

The Euler-Euler approach was employed to simulate gas-liquid two phase flow in aluminum reduction cells, whereby the continuous and disperse phases are considered as interpenetrating media, identified by their local volume fractions. In this work, the Euler-Euler model involving continuity and momentum equations for both phases is identical to that reported in our previous work [15]. The momentum exchange term used in our model was Schiller-Naumann-Pb. Here, due to the limited space, most of the model equations were listed as supplementary data. A modified k-ε turbulence model was used to describe liquid phase turbulence in the simulation, using the standard k-ε model supplemented with extra terms that include the inter-phase turbulent momentum transfer and Tchen-theory correlations for the dispersed phase [16].

The population balance model

The population balance equation (PBE) is the conservation equation of the number n_i of the bubbles (per unit volume) of size i used computational fluid dynamics methods and added the population balance modeling. In this work, a class method(CM) is used to simplify the PBE so as to realize the combination of the CFD model and PBM model, which are then both solved interactively by the commercial CFD code ANSYS FLUENT. For coalescence and breakage only, the CM equation for the size i is given by:

$$\frac{\partial n_i}{\partial t}+\nabla\cdot\left(U_G\cdot n_i\right)=B_B-D_B+B_C-D_C \tag{1}$$

where B_B, D_B, B_C, and D_C, respectively, represent the birth rate due to breakage of larger bubbles, the death rate due to the breakage into smaller bubbles, the birth rate due to the coalescence of smaller bubbles and the death rate due to the coalescence with other bubbles. These different rates can be expressed in [17]. By defining the bubble size fraction as $f_i=\left(\alpha_i/\alpha_g\right)$ and assuming that all size groups share the same density and velocity, so we can obtain the following equation:

$$\frac{\partial}{\partial t}\left(\rho_g\alpha_g f_i\right)+\frac{\partial}{\partial x}\left(\rho_g\alpha_g f_i\vec{u}_g\right)=S_i \tag{2}$$

where ρ_g, α_i, α_g , u_g, S_i, respectively, represent the density of anodic bubble, the volume fraction of bubble size i, the total volume fraction of bubble and the source of PBE.

The closure used for PBM in the following study is the closure for aggregation and breakage by Luo and Svendsen model, considering the coalescence only induced by turbulence eddies and the breakage only due to isotropic turbulence. According to the electrolytic test results of Poncsak and Cassayre [18-19], the size of initial bubble and the largest bubble were about 1mm and 40mm, so the diameters are divided into 16 classes with user customed size as described in Table1:

Table 1 The sizes of discrete bubble classes

Class	Bin diameter (mm)	Class	Bin diameter (mm)
1	1	9	10
2	1.5	10	12
3	2	11	14
4	3	12	17
5	4	13	20
6	5	14	24
7	6	15	29
8	8	16	35

Simulation conditions and CFD modeling strategy

This study is mainly trying to solve the effects of current density, anode width and the presence of slots on the bubble size distribution which neglects the influence of electromagnetic force. Therefore, only a simplified geometric model (one anode) was established because it may take a lot of computing resource for the PBE. The widths of the inter-anode channel, the side one, the end one, the center one and anode-cathode distance are 40mm, 250mm, 300mm, 200mm and 40mm, respectively. The main physical parameters used in this computation were shown in Table 2. In the simulation, the top of the bath was treated as degassing boundary condition and anode bottom was treated as gas mass flow inlet boundary condition, where the size of initial bubbles was 1mm. No-slip wall was used for bath phase and free-slip wall was used for bubble phase. The basic assumption for coupling CFD and PBM is that bubbles of all sizes share a common velocity field through coupling the Sauter diameter (d_{32}) to the drag term.

$$d_{32}=\frac{\sum_{i=1}^{N}N\cdot d_i^3}{\sum_{i=1}^{N}N\cdot d_i^2} \tag{3}$$

Table 2 The physical parameters of the computational model

	Density(kg/m^3)	Dynamic viscosity(Pa·s)	Surface tension(N/m)
Bath	2130	2.51×10^{-3}	0.134
Bubble	0.398	5.05×10^{-5}	

Results and discussion

In the present work, the CFD-PBM model for predicting the bubble size distribution in aluminum reduction cells was established by using proper bubbles coalescence and breakage mechanism. In a given gas-liquid two phase system, bubbles coalescence and breakage rates are mainly affected by the local bubble volume fraction and bath turbulent dissipation rate. As the bubbles mainly exist under the anode bottom, actually, the bubble size distribution in those regions is one of the most concerning problems in aluminum industry, because it is closely related with function of cell design and operation parameters. So we choose three important parameters, i.e., current density, anode width and

slot configuration, all of which can affect the number and the size distribution of the bubbles. For description convenience, four different heights of z-section in ACD were defined, which stands for distance from the anode bottom. These z-sections were named as z-4mm, z-8mm, z-12mm and z-16mm, respectively.

The effect of current density

The bubble size distribution in ACD with different current densities is shown in Fig.1. It is can be seen that a large number of small size bubbles coexist with a few numbers of medium size and large size bubbles at certain current density. Not only this, the correlation between the number of bubbles and bubble diameter has nearly a hyperbolic shape. The size of the largest number of bubbles is less than 5mm, but the numbers of medium and large bubbles are 1 to 2 orders of magnitude lower than small bubbles. This is because in our CFD-PBM model the size of all the bubble is assumed to be 1mm at the gas inlet boundary, which was accordance with the size of initial bubble generated under anode bottom. The formation of large bubbles is due to a large number of coalescence of small and medium bubbles when bubbles move under anode bottom. This is in good agreement with the bubble size distribution found in the literature [6, 18, 20].

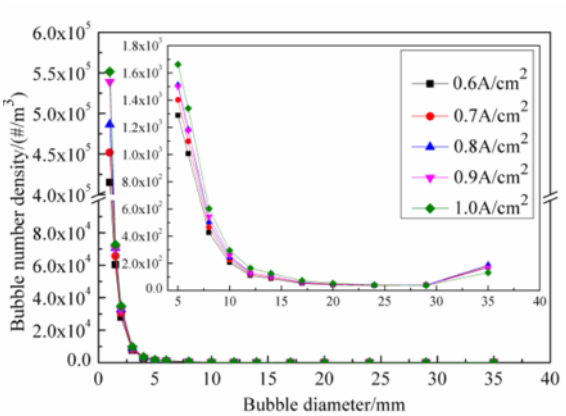

Fig.1 Bubble size distribution in ACD with different current densities

As shown in Fig.2, the average bubble volume fraction increases in ACD with the increase of current density. According to Faraday's Law, with current density increases, gas flow flux would also increase, which results in a higher generation rate. Fig.3 shows that average bath turbulent dissipation rate decreases with the increase of current density. From Figs.2-3, it can be observed that the average bath turbulent dissipation rate decreases with the increase of average bubble volume fraction, due to complex flow field related with modified k-ε turbulence model. The farther away from the anode bottom, both lower are the average bubble volume fraction and the average bath turbulent dissipation rate. Unlike the average bubble volume fraction, the trend for the average bath turbulent dissipation rate is reduced.

Fig.4 shows the average bubble Sauter diameter decreases with the increase of current density. It can also be seen from Fig.1 that the proportion of small bubbles will increase if current density increase. On the other hand, the coalescence and breakage of bubbles mainly occur under the anode bottom, where the bath turbulence intensity is very low. This fact indicates that the rate of coalescence of bubbles have not changed so much as the current density increases. When the current density is over approximately 0.8A/cm^2, the diminution of average bubble Sauter diameter becomes more obviously.

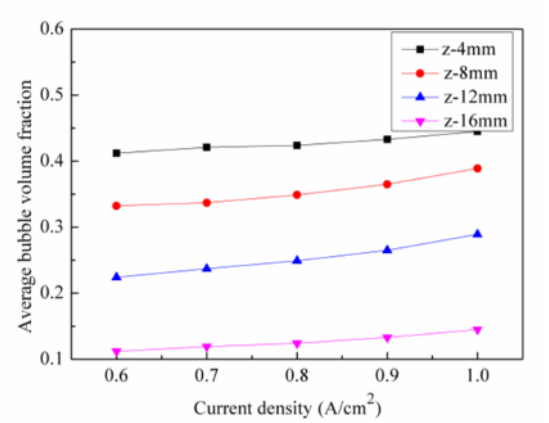

Fig.2 Average bubble volume fraction in ACD with different current densities

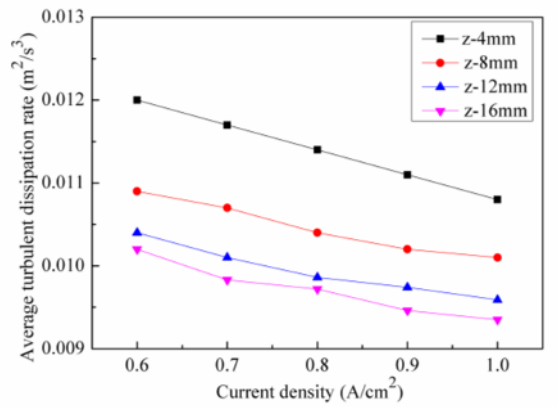

Fig.3 Average turbulent dissipation rate in ACD with different current densities

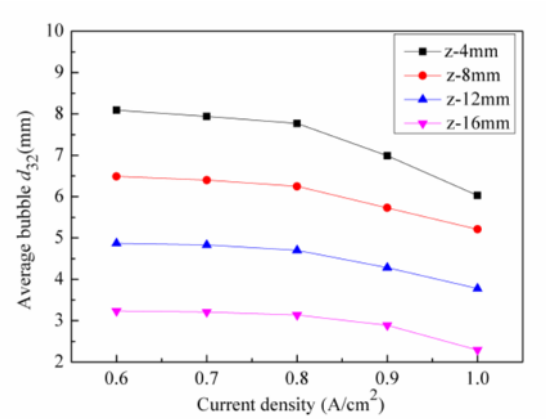

Fig.4 Average bubble d_{32} in ACD with different current densities

The effect of anode width

The anode width is one of the most important parameters for aluminum reduction cells. To investigate the effect of anode width on the bubble size distribution, four anode widths are studies, i.e.,

500mm, 550mm, 600mm and 650mm. The simulation results are shown in Figs.5-8.

Fig.5 shows that the average bubble volume fraction at different z-sections increases with the increase of the anode width. The bubbles have to travel a longer path if the anode width is large. So more and more bubbles stay at the anode bottom, leading to an increase of the accumulated bubbles. At the same time, from Fig.6, the bath turbulent dissipation rate decreases with the increase of anode width. Because the bubble flow form has an effect on the bath flow field, as a result, a larger anode width will reduce the intensity of bath velocity field and turbulent dissipation rate will also decrease. Fig.7 shows the average bubble Sauter diameter increases with the increase of the anode width. As we know that the coalescence and breakage of bubbles are mainly due to the combination of volume fraction and turbulent dissipation rates in our CFD-PBM model. The chance of coalescence between smaller bubbles will increase if the bubble volume fraction is high and the chance of breakage from larger bubbles will decrease if the dissipation rate is low.

Fig.8(a), (b), (c) and (d) shows the bubble Sauter diameter distribution at z-8mm in ACD with different anode widths. The large bubbles mainly stay at the middle compartment of anode bottom. As the anode width increases, the bubble Sauter diameter increases and the area of the large bubble region increases too; in addition, the large bubbles distribution seems to be more uniform.

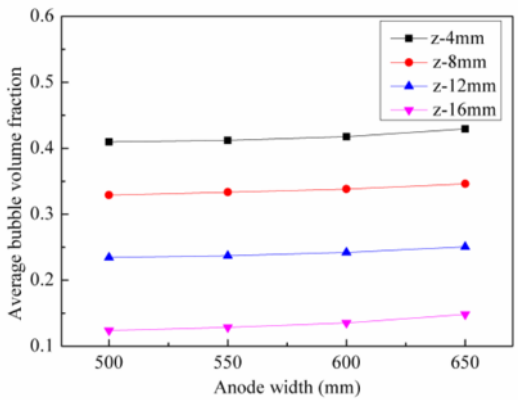

Fig.5 Average bubble volume fraction in ACD with different anode widths

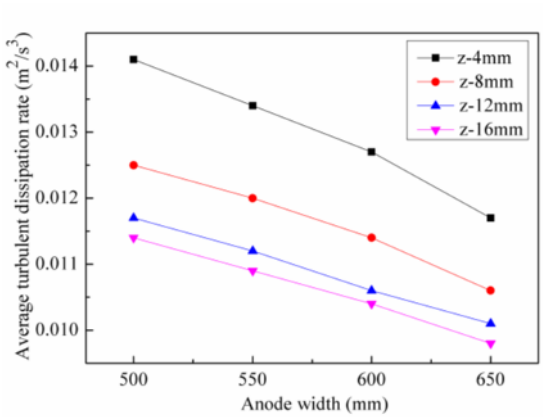

Fig.6 Average turbulent dissipation rate in ACD with different anode widths

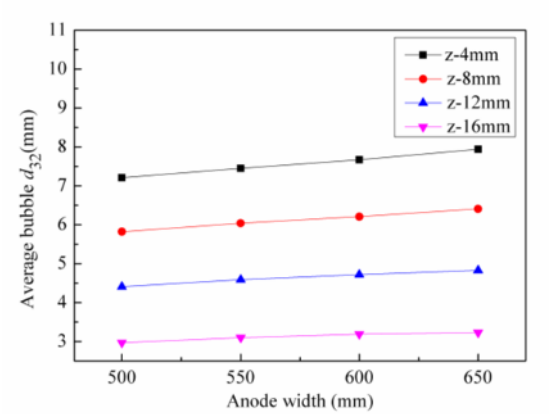

Fig.7 Average bubble d_{32} in ACD with different anode widths

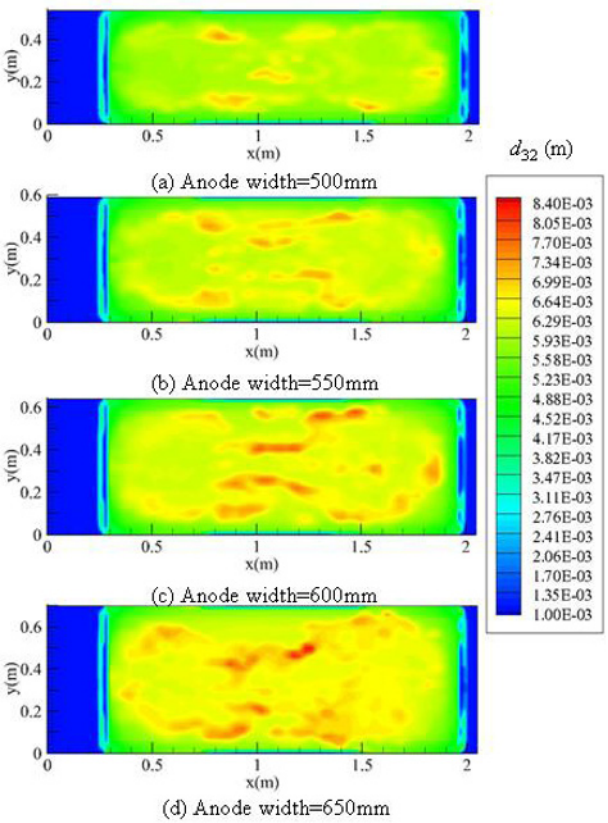

Fig.8 Bubble d_{32} distribution contours in ACD (z-8mm) with different anode widths

The effect of slot configuration

It is well known that the anodes with slots can reduce the voltage drop and noise due to anodic bubbles, which can escape more quickly from the anode bottom. In this work, the effect of slot configuration on the bubble size distribution in aluminum reduction cells has been investigated based on bubble volume fraction and turbulent dissipation rate in ACD.

Figs. 9-11 show the effect of slot configuration on the average bubble volume fraction, the average turbulent dissipation rate and the average bubble Sauter diameter at different z-sections in ACD.

Because the slots are acting as an additional inter-anode gap, where the bubbles escape vertically from the anode bottom, and the bubble residence time gets short. Therefore, the average bubble volume fraction is lower under the bottom of anodes with slots than the ones without slots. Conversely, bath turbulent dissipation rate induced by the bubble increases more intensely in the anodes with slots. As a result, it is more likely that the chance of coalescence between smaller bubbles would reduce but the chance of breakage from larger bubbles increases. So the average bubble Sauter diameter is smaller in the model of anodes with slots.

Fig.12(a), (b)and(c) shows the bubble Sauter diameter distribution at z-8mm in ACD under normal anodes, anodes with one slot and anodes with two slots respectively. We can see that the local bubble size distribution is more uniform and the proportion of large bubbles reduces obviously in the anodes with slots. It can be seen from Fig.12(b) and (c) that, as the larger the number of such slots, the above phenomenon is more obvious. From Fig.12(c), the size of Sauter diameter is about 5mm and the Sauter diameter assumes a uniform distribution under the anodes with two slots.

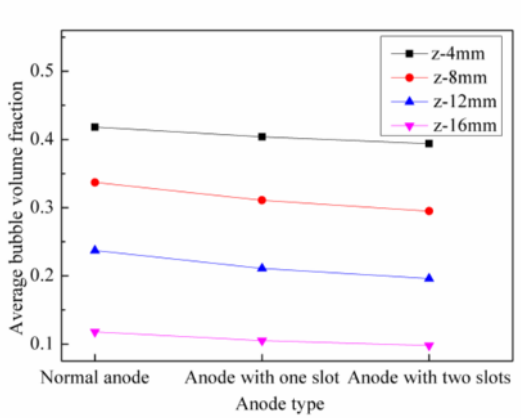

Fig.9 Average bubble volume fraction in ACD with different types of slot configuration

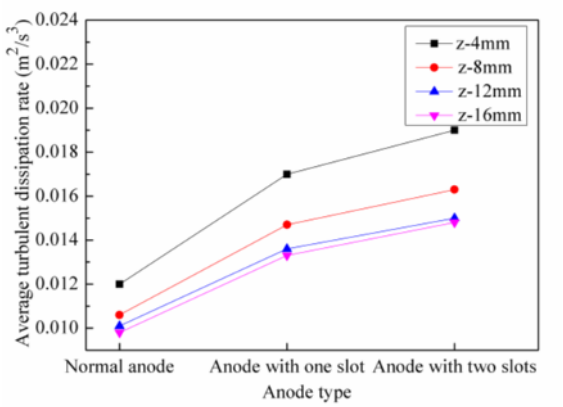

Fig.10 Average turbulent dissipation rate in ACD with different types of slot configuration

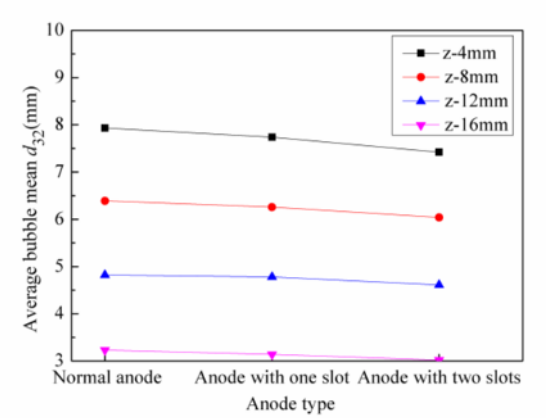

Fig.11 Average bubble d_{32} in ACD with different types of slot configuration

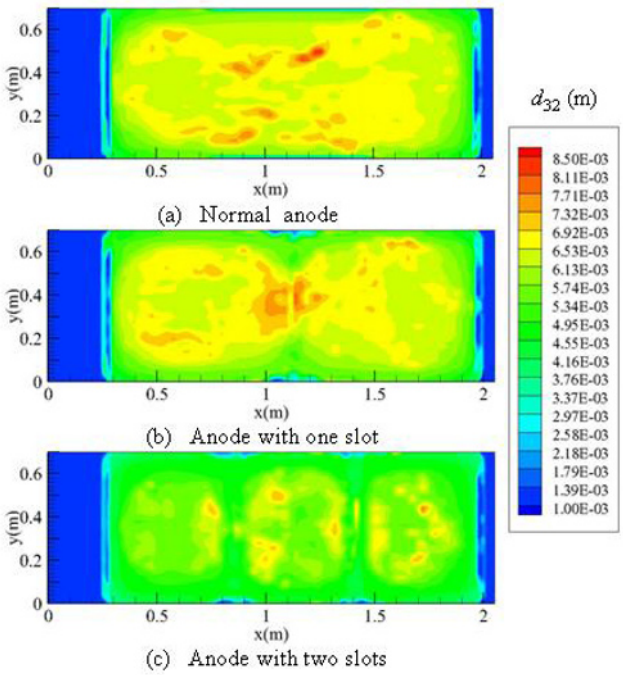

Fig.12 Bubble d_{32} distribution contours in ACD (z-8mm) with different types of slot configuration

The effect of the MHD

The MHD and bubbles driving forces both have an important impact on the bath flow in the real industrial aluminum reduction cells. We will see that the bath flow fields, i.e., the bubble volume fraction and the turbulent dissipation rate, have an important effect on the bubble size distribution under the anode bottom. Since the MHD can exist any location in a full cell model, some large eddies can be formed. But unlike the MHD, the bubbles generated on each anode move in separate regions and form a series of small eddies. The bubble volume fraction and the turbulent dissipation rate in the model with the MHD and bubbles forces could be different from that without the MHD. Therefore, bubble size distribution which has an important relationship with these two main flow factors should be different when considering the influence of the MHD.

Conclusions

In this study, a CFD-PBM coupled model was developed to describe the bubble size distribution in aluminum reduction cells, in which the coalescence and the breakage of bubbles were considered. And the effects of current density, anode width and the presence of slots on the bubble size distribution have been investigated.

It is found that a large number of small size bubbles coexist with a small numbers of medium size and large size bubbles at certain current density and the correlation between the number of bubbles and bubble diameter has nearly a hyperbolic shape. The numbers of medium and large bubbles are 1 to 2 orders of magnitude lower than small bubbles.

The average bubble Sauter diameter decreases with the increase of current density and increases with the increase of anode width; and the average bubble Sauter diameter is smaller in the model of anodes with slots.

The bubble volume fraction and the turbulent dissipation rate have an important effect on the bubble size distribution under the anode bottom. They help to determine the probability or rate of coalescence and breakage mechanism of anodic bubbles.

The importance of the research on the MHD for the bubble size distribution is discussed. The model with the MHD and bubbles driving forces coupled could be further used to study the bubble size distribution. This will be next step in our study.

Acknowledgment

The authors thank High-tech Research and Development Program of China (2010AA065201), CHALCO Ltd (ZB2013CBBCe1), the National Natural Science Foundation of China(50974127) and the Fundamental Research Funds for the Central Universities of Central South University (2013zzts038).

References

1. Fortin S., Gerhardt M., and Gesing A J., Physical modeling of bubble behaviour and gas release from aluminum reduction cell. Light Metals 1984, 721-741.
2. Solheim A., and Thonstad I., Model Cell Studies of Gas Induced Resistance in Hall-Heroult Cells. Light Metals 1986, 397-403.
3. Xiang-peng L., Jie L., Yan-qing L., Heng-qin Z., and Ye-xiang L., Physical modelling of gas induced bath flow in drained aluminium reduction cell. Trans. NonferrousMet. Soc. China, 14 (2004), 1017-1022.
4. Qian K., Chen Z D., and Chen J J., Bubble coverage and bubble resistance using cells with horizontal electrode. Journal of Applied Electrochemistry, 28 (1998), 1141-1145.
5. Chen J J., Qian K., and Zhao J C., Resistance due to the presence of bubbles in an electrolytic cell with a grooved anode. Institution of Chemical Engineers, 79 (2001), 383-387.
6. Alam M., Morsi Y., Yang W., Mohanarangam K., Brooks G., and Chen J J., Investigation of electrolytic bubble behaviour in aluminum reduction cell. Light Metals, 2013, 591-596.
7. Nai-jun Z., Yu-qing X., Chen J J., and Taylor M. P., Numerical simulation of electrolyte two-phase flow induced by anode bubbles in an aluminum reduction cell. Chemical Product and Process Modeling, 11 (2007), 1934-1945.
8. Kai-yu Z., Yu-qing F., Schwarz P., Cooksey M., and Zhao-wen W., Numerical investigation of bubble dynamics in aluminium electrolytic cells. Light Metals, 2012, 881-886.
9. Hong-liang Z., Zhi-gang W., Jie L., and Yan-qing L., Simulation on flow field of anode gas and electrolyte in aluminum electrolysis with cermet inert anodes. Journal of Central South University (Science and Technology), 41(2010), 1256-1262.
10. Xiao-xia X., Nai-jun Z., and Da-guang C., Numerical simulation on two phase flow field of electrolyte in 156 kA aluminum reduction cells. The Chinese Journal of Nonferrous Metals, 16(2006), 1988−1992.
11. Chen P., Dudukovic M P., and Sanyal J., Three-dimensional simulation of bubble column flows with bubble coalescence and breakage. AICHE J., 51(2005), 696-712.
12. Prince M J., and Blanch H W., Bubble coalescence and break-up in air-sparged bubble columns. AIChE J., 36(1990), 1485-1499.
13. Luo H., and Svendsen H F., Theoretical model for drop and bubble breakage in turbulent dispersions. AIChE J., 42(1996), 1225-1233.
14. Lehr F., Milies M., and Mewes D., Bubble size distribution and flow fields in bubble columns. AIChE J., 48 (2002), 2426-2443.
15. Shui-qing Z., Jie-min Z., Mao L., Yi-wen Z., and Jian-hong Yang., Numerical simulation of gas-liquid two-phase flow in aluminum reduction cells with perforated anodes. CIESC Journal. 10 (2013), 3612-3619.
16. Ansys Fluent 6.3. User Manuals. Fluent Inc, 2007.
17. Luo H., Coalescence, Breakage and Liquid Circulation in Bubble Column Reactors, (Ph.D. thesis, Norwegian Institute of Technology, 1993),
18. Poncsak S., Kiss L I., Toulouse D., Perron A., and Perron S., Size distribution of the bubbles in the Hall-Heroult cells. Light Metals, 2006, 457-462.
19. Cassayre L., Utigard T A., and Bouvet S., Visualizing gas evolution on graphite and oxygen-evolving anodes. JOM., 54(2002), 41−45.
20. Kiss L I., Ponesak S., and Antille J., Simulation of the bubble layer in aluminum electrolysis cell. Light Metals, 2005, 559-564.